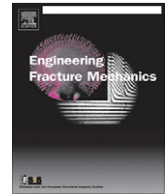




ELSEVIER

Contents lists available at SciVerse ScienceDirect

## Engineering Fracture Mechanics

journal homepage: [www.elsevier.com/locate/engfracmech](http://www.elsevier.com/locate/engfracmech)

## Three-dimensional simulation of fretting crack nucleation and growth

B.J. Carter<sup>a,b,\*</sup>, E.C. Schenck<sup>c</sup>, P.A. Wawrzynek<sup>a,b</sup>, A.R. Ingraffea<sup>b</sup>, K.W. Barlow<sup>d</sup><sup>a</sup> Fracture Analysis Consultants, Inc., 121 Eastern Heights Drive, Ithaca, NY 14850, USA<sup>b</sup> Cornell Fracture Group, Room 643 Rhodes Hall, Cornell University, Ithaca, NY 14851, USA<sup>c</sup> Impact Technologies, LLC, 200 Canal View Blvd., Rochester, NY 14623, USA<sup>d</sup> Naval Air Systems Command, Propulsion and Power Engineering, NAVAIR, 22195 Elmer Road, Building 106, Patuxent River, MD 20670, USA

## ARTICLE INFO

## Article history:

Received 27 December 2011

Received in revised form 20 July 2012

Accepted 15 August 2012

## Keywords:

Fretting

Finite element analyses

Crack growth

Life prediction

Metals

## ABSTRACT

Fretting nucleation models and three-dimensional finite element analyses are used to compute the fretting fatigue life for metallic components. The models predict crack nucleation cycles and location(s). Discrete crack growth simulations provide stress intensity factor histories, with multiple, non-planar, three-dimensional cracks possible. The histories are input into crack growth rate model(s) to compute propagation cycles. The sum of fretting nucleation plus propagation cycles is the total life. Experimental fretting data, including crack nucleation location and cycles, and crack growth trajectory and propagation cycles, are used to validate the approach. Predictions for a realistic turbine blade/disk are comparable to field observations.

© 2012 Elsevier Ltd. All rights reserved.

## 1. Introduction

Fretting fatigue can be a controlling factor in the life of some aircraft engine components, such as turbine blade/disk assemblies [1,2]. Fretting also occurs at threaded joints [3,4], in gears and shafts [5,6], and in wheel/axle assemblies [7] – essentially wherever two parts are in forced-contact and subject to cyclic loading with the occurrence of limited slip between the two parts. The analysis of fretting in turbine engines can be rather complicated due to the loading and temperature variations, complex component geometry, anisotropic material properties, residual stress, and non-trivial crack geometry, which might include multiple, interacting/branching, non-planar cracks. Although engine components are designed to minimize fretting fatigue [8,9], it often still occurs, leading to possible premature or catastrophic failure due to fretting induced discrete crack nucleation and growth.

A growing number of technical journal articles are devoted to fretting fatigue, and in particular, to the development and validation of fretting fatigue crack nucleation models [4,6,10–18]. Typically, fretting nucleation models are based on experimental observations and analytical, semi-analytical or finite element predictions of the contact stress and/or strain near the edge of contact (EOC). These nucleation models generally predict the number of cycles to nucleate a crack, and some also predict the location and orientation of the initial crack.

The EOC is typically a region of high stress (and strain) and a common site for fretting crack nucleation. Closed-form solutions for the stress in the contact region have been developed for some simple cases, such as sphere-on-flat or cylinder-on-flat geometries [19]. Approximate numerical techniques, such as singular integral equations [20,21] or finite element (FE) methods [7,14,22] are used when closed-form solutions are not possible or practical. FE modeling of the contact region requires non-linear solution strategies, special elements or constraints on the contact surface, and a sufficiently refined mesh to capture the potentially singular stresses at the EOC.

\* Corresponding author at: Fracture Analysis Consultants, Inc., 121 Eastern Heights Drive, Ithaca, NY 14850, USA.

E-mail address: [bjc21@cornell.edu](mailto:bjc21@cornell.edu) (B.J. Carter).

## Nomenclature

$\sigma_{eq}$	equivalent stress fretting model parameter
$\gamma_{crit}$	critical shear stress fretting model parameter
$\Gamma_{crit}$	Smith–Watson–Topper fretting model parameter
$Q$	RAI's crack analog fretting model parameter
$N_f$	number of load cycles for fretting crack nucleation
$P$	normal load on fretting test specimen
$S_{max}$	maximum tangential load on fretting test specimen
$S_{min}$	minimum tangential load on fretting test specimen
EOC	Edge of contact
LE	Leading edge of contact
TE	Trailing edge of contact
$da/dN$	Crack growth per cycle
$K_{min}$	minimum Mode I stress intensity factor
$K_{max}$	maximum Mode I stress intensity factor
$K_{eff}$	effective Mode I stress intensity factor
$K_{th}$	threshold Mode I stress intensity factor
$R$	ratio of $K_{min}/K_{max}$
SIF	stress intensity factor

Various stress- and strain-based fatigue models have been used quite successfully to predict fretting fatigue crack nucleation cycles and crack location [11–14]; the critical plane versions of these models also predict the initial crack orientation. Lykins et al. [23] evaluated a number of these models using experimental data, and then proposed a new model that uses the critical plane shear stress amplitude [13]. This new model has been used successfully to compute the number of cycles to nucleation as well as the location and orientation of the initial crack in experiments. Another model is based on an equivalent stress parameter [12,24]; this model does not provide crack orientation, but has been used successfully to predict the crack nucleation location and nucleation cycles.

These stress- and strain-based models are often found to be conservative as they under-predict the number of cycles to nucleation. Moreover, they lack a length scale. To account for these issues, averaging over a small distance or volume can be performed [4,25,26]; this concept can be related to the nonlinear process zone at a crack front. Borrowing further from fracture mechanics, another class of fretting nucleation models, called notch- or crack-analog models [4,15–18,27], have been developed. The various analog models differ primarily in the handling of friction, slip and geometry effects. The analog model developed by Ahmad and Santhosh [16] avoids some of these issues by computing the nucleation parameter under bonded conditions.

Fretting crack nucleation generally leads to discrete crack growth. Typically, the crack growth is divided into two stages [18,28]; the first stage is inclined growth from the surface near the EOC, driven by shear stress on the contact surface, and the second stage is growth that is roughly perpendicular to the contact surface and dominated by the bulk tensile stress. Studies of fretting crack nucleation and propagation have been performed using analytical and FE techniques [12,29–33]. Mostly, these analyses have been limited to two-dimensions (2D) or constrained to simplified three-dimensional (3D) planar, semi-elliptical cracks.

A typical crack growth simulation starts from an initial crack; thus, the initial nucleated crack size must be defined. During laboratory testing, fretting nucleation cycles are counted until a crack is nucleated, after which crack propagation cycles are counted. The sum of the two represents the total fretting fatigue life of the component. Lykins et al. [13] defined the initial crack size based on typical eddy-current detection limits ( $760 \times 380 \mu\text{m}$ ), and then computed nucleation and propagation lives by counting striations on fracture surfaces. Golden and Calcaterra [34] define the initial crack to be  $25 \times 125 \mu\text{m}$ , based on fractographic analyses. Navarro et al. [35,36] developed a model that does not require a strict definition of the initial crack size; instead the initial crack size is determined from the combination of the nucleation and propagation rates.

By combining the fretting fatigue crack nucleation cycles with discrete crack growth cycles, an analyst can predict the total life of a component that is subject to fretting fatigue. From the authors' perspective, a shortcoming of the above studies has been the simplified fracture mechanics and crack growth analyses that have been performed (either 2D or simplified 3D crack shapes). One exception to this is the work of Pierres et al. [37] who used the extended finite element method (XFEM) to simulate 3D cracking observed during a sphere-on-plate fretting fatigue test.

This paper describes a new approach for simulating, in 3D, both fretting nucleation and discrete crack propagation using standard finite element analysis capabilities of ANSYS [38] and FRANC3D [39]. The combined software allows an analyst to use one or more of the available fretting nucleation models to predict fretting crack nucleation cycles as well as location and orientation of the initial crack(s). Subsequent discrete 3D crack growth simulations can then be performed to compute stress intensity factor (SIF) histories, which are used to determine crack propagation cycles.

The fretting nucleation, crack growth, fatigue life models and the software are briefly described in the next section. The software and simulation approach are validated using experimental and field data obtained from the literature, as described in Section 3, while Section 4 discusses the stochastic nature of this data and the range of numerical predictions provided by the models and the software.

## 2. Fretting fatigue analysis methodology

### 2.1. Analysis software

Fretting fatigue can be simulated using standard FE analysis capabilities. For instance, ANSYS [38] is widely used in industry to perform stress analyses of turbine engine components, and includes capabilities for modeling contact between mating parts. The FE analysis provides the displacement, stress, strain and contact information. These results along with the FE model itself are passed along to FRANC3D [39] for fretting and discrete crack analysis. In addition to discrete crack growth capabilities, FRANC3D now includes fretting fatigue crack nucleation models, which are used to predict the fretting cycles and the initial crack geometry, specifically the size, location and possibly orientation of the crack(s).

### 2.2. Fretting crack nucleation

To observe and measure fretting fatigue, simple coupon-type testing is often conducted. A typical fretting test consists of a specimen and pads as shown in Fig. 1. A constant normal load ( $P$ ) is applied to the fretting pads, and then the specimen is subjected to a cyclic axial load ( $S_{max}-S_{min}$ ), which produces shear between the specimen and the pad. Fretting crack nucleation occurs after a sufficient number of load cycles.

The usual result of such fretting fatigue experiments is a plot, similar to Fig. 2, where the number of cycles to crack nucleation is plotted against a fretting parameter,  $f_p$ . The data is typically fit to an equation of the form:

$$f_p = aN_i^b + cN_i^d \quad (1)$$

This equation then is used to determine the number of cycles to nucleation,  $N_i$ , given  $f_p$  and the four coefficients:  $a-d$ . The coefficients are material dependent and defined by the fretting nucleation model.

Four fretting nucleation models have been implemented in FRANC3D: the equivalent stress [12,24], the critical plane shear stress amplitude [13], the critical plane Smith–Watson–Topper [11,23], and a crack-analog model [16]. The model equations and parameters are briefly summarized here.

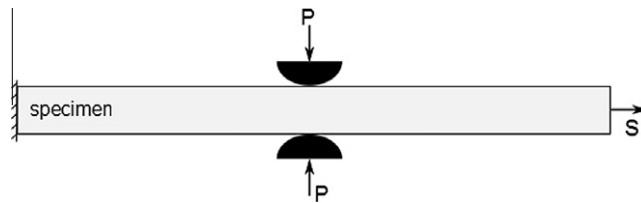


Fig. 1. Schematic of a typical fretting fatigue experiment.

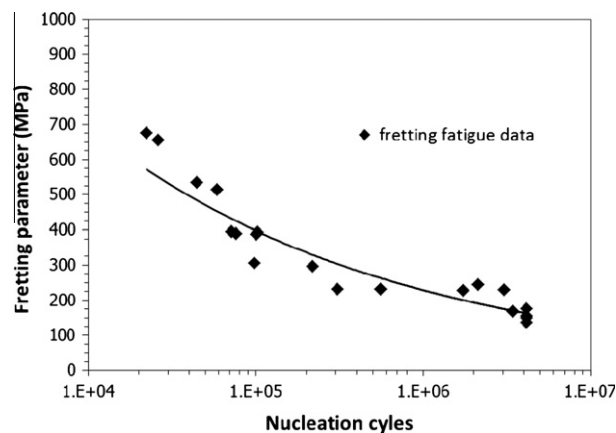


Fig. 2. Typical fretting fatigue experimental test data (adapted from [40]).

The equivalent stress model is defined by:

$$\sigma_{eq} = 0.5(\Delta\sigma_{psu})^w (\sigma_{max})^{1-w} \quad (2)$$

where  $\Delta\sigma_{psu}$  and  $\sigma_{max}$  are functions of the nodal stress components and  $w$  is a material dependent fitting parameter. Based on curve fitting of experimental data, the equation, in the form of (1):

$$\sigma_{eq} = aN_i^b + cN_i^d \quad (3)$$

relates  $\sigma_{eq}$  to  $N_i$ , where coefficients  $a$ – $d$  are material dependent fitting parameters. For example, for Ti–6Al–4V,  $a = 52476$ ,  $b = -0.6471$ ,  $c = 450.85$  and  $d = -0.03582$  [24].

The critical plane shear stress amplitude model is defined by:

$$\gamma_{crit} = \tau_{max}/G(1 - R_\tau)^m \quad (4)$$

where  $\tau_{max}$  is the maximum shear stress on the critical plane,  $R_\tau$  is the shear stress ratio,  $G$  is the shear modulus and  $m$  is a material dependent fitting parameter. Substituting  $\gamma_{crit}$  for  $\sigma_{eq}$  in Eq. (3), one can compute  $N_i$  given the appropriate values for the coefficients  $a$ – $d$ . For Ti–6Al–4V,  $a = 6.46$ ,  $b = -0.686$ ,  $c = 4.65 \times 10^{-3}$  and  $d = 1.22 \times 10^{-2}$  [40].

The critical plane Smith–Watson–Topper model is defined by:

$$\Gamma_{crit} = \sigma_{max}(\Delta\varepsilon/2) = (\sigma_f^2/E)(2N_i)^{2b} + \varepsilon_f(2N_i)^{b+c} \quad (5)$$

where  $\sigma_{max}$  is the maximum principal stress and  $\Delta\varepsilon$  represents the normal strain amplitude on the critical plane; this equation is already in the form of Eq. (3).  $E$  is the elastic modulus,  $\sigma_f$  and  $\varepsilon_f$  are material strength parameters, and  $b$  and  $c$  are fitting parameters. For Ti–6Al–4V,  $\sigma_f = 376.6$  MPa,  $b = 1.78 \times 10^{-4}$ ,  $c = -0.767$  and  $\varepsilon_f = 32.4$  [40].

The crack analog model is quite different from the above three models. First, the fretting parameter ( $Q$ ) is only computed at the nodes along the EOC. Second, the FE analysis must be conducted with bonded contact conditions rather than the standard contact (that allows for slip and requires a coefficient of friction).  $Q$  can be related to  $J_{II}$  from linear elastic fracture mechanics [16]:

$$Q = (J_{II}E/(1 - \nu^2))^{1/2} \quad (6)$$

where  $\nu$  is Poisson's ratio.  $N_i$  is computed from:

$$\log N_i = (\alpha - \Delta Q)/\beta \quad (7)$$

where  $\alpha$  and  $\beta$  are material dependent fitting parameters.  $\Delta Q = Q_{max} - Q_{min}$ , is determined from the maximum and minimum load cycles.

An uncracked FE model along with displacement, stress, strain and contact status results is used to compute fretting nucleation. Contact surfaces are automatically determined from the FE model data and the contact status, and the EOC then is determined from the boundary of the contact surfaces. The analyst can choose one (or more) of the four fretting nucleation models described above to compute  $N_i$  and the initial crack location (and possibly the initial crack orientation). For every FE node on the contact surface, the nodal displacement vector along with the stress and strain tensors are extracted from the imported analysis results. These results are processed to determine the value of the chosen fretting model parameter and the corresponding  $N_i$ . Crack nucleation is predicted to occur at the location where  $N_i$  is the minimum.

Note that the  $N_i$  versus  $f_p$  curve fit is based on experimental data, where cycles are counted until crack nucleation occurs. This implies that a nucleation crack size is pre-defined, and crack growth simulations can start from this initial crack size.

### 2.3. Fretting crack propagation

Discrete crack propagation starts from the initial fretting crack. A small portion of a FE model can be extracted from a full model and imported into FRANC3D, where crack nucleation and growth is performed. The cracked and remeshed sub-model is recombined with the rest of the model and then analyzed; this means that the solution includes all the relevant boundary conditions and accounts for any load path changes as the crack grows. The process is illustrated in Fig. 3 using a mini-turbine disk test specimen [41]; a small portion of the disk is extracted, cracked, remeshed and then recombined with the full model for analysis. The mesh facets and nodes on the cut-surface are retained to maintain compatibility with the full model.

A fretting fatigue analysis is complicated by the contact conditions, multiple load cases, and multiple material regions. Typically, a crack is inserted within or near the edge of original contact surface in one of the regions. The contact surface is automatically redefined after crack insertion and after each step of crack growth because the surface-mesh adjacent to the crack mouth changes. In addition, contact conditions on the crack surface are automatically generated if the analysis requires it, which occurs if the minimum load case ( $S_{min}$ ) is negative and causes crack closure.

At each step of crack growth, the cracked local portion is joined with the global portion of the model and a full FE stress analysis is performed. The simulation ultimately produces a series of crack fronts and associated SIFs along the fronts. A SIF history is extracted by following a path that intersects successive crack fronts. This SIF history is required to compute crack propagation cycles as described in the next section.

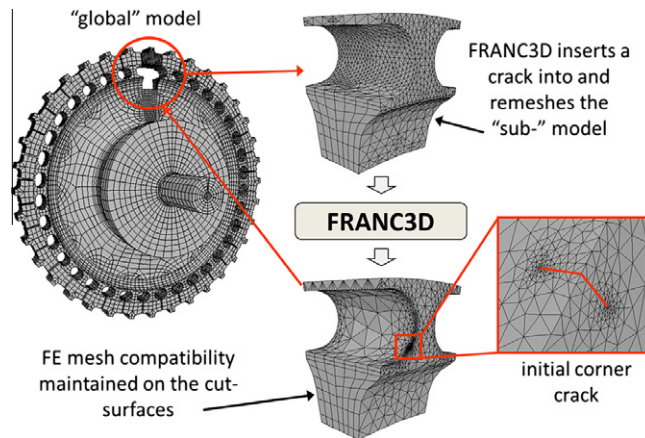


Fig. 3. FRANC3D sub-modeling approach [39].

#### 2.4. Fretting fatigue life

The fatigue life of a component that is subject to fretting is the sum of the fretting nucleation cycles plus the crack propagation cycles. The fretting nucleation cycles are computed from the chosen fretting nucleation model (see Section 2.2). The discrete crack propagation cycles are computed based on the SIF history and a crack growth rate model. Several crack growth rate models are available, including the Paris [42], NASGRO [43] and AFRL [34] equations. Using the selected growth rate model, SIF history and appropriate material dependent data, the propagation cycles are computed and then added to the fretting nucleation cycles to determine the total life.

### 3. Fretting fatigue simulation results

The analysis approach and software described in Section 2 is used to simulate fretting fatigue in both test specimen and actual turbine-engine parts. A typical fretting test specimen is simulated first to validate the fretting nucleation models and the software implementation. A second fretting test specimen, which more closely resembles turbine-engine blade/disk connections, is simulated next to validate the fretting nucleation models, the discrete crack growth and the total fatigue life computations. The third model represents actual turbine-engine blade/disk geometry and provides additional validation.

#### 3.1. Analysis of dog-bone specimens

The software described in Section 2 is used to compute fretting crack nucleation cycles and locations in standard fretting coupon tests of dog-bone specimens with round indenters [13,23]. A sketch of the fretting test specimen and pad is shown in Fig. 4. The leading EOC (LE) and trailing EOC (TE) are shown to help locate the crack nucleation site(s).

A 3D FE model of the fretting specimen and pad is built using ANSYS, taking advantage of symmetry through the specimen thickness so that only one fretting pad is modeled. A sample of five of Lykins' fifty test cases are analyzed here; all use the same geometry and the same normal load ( $P$ ) but with varying  $S_{max}$  and  $S_{min}$ , Table 1. The loads are applied using three load cases. First,  $P$  is applied (see Fig. 1), and then held constant at 1.3 kN. Second,  $S_{max}$  is applied to the fretting specimen (see Fig. 1). The final load case ramps the axial stress down from  $S_{max}$  to  $S_{min}$ .  $Q_{max}$  and  $Q_{min}$  values in Table 1 are the measured tangential reaction forces on the fretting pad. The fretting specimen and pad are both Ti-6Al-4V; the elastic modulus is 126.1 GPa, Poisson's ratio is 0.34, and the coefficient of friction on the contact surface is set to 0.5.

For each test case, Lykins calculated values for the  $\gamma_{crit}$  and  $\Gamma_{crit}$  fretting models. Although Lykins does not provide predicted  $N_i$  values for each specimen and nucleation model, he does report  $a \pm 3N_i$  scatter between experimental and predicted nucleation cycles, for the lower range of  $N_i$  values. The predicted  $N_i$  values fall within these bounds, and are similar to Lykins' experimental (exp) results for  $N_i$  as shown in Tables 2 and 3. The last column in Tables 2 and 3 show the ratio between the predicted and experimental  $N_i$  values; all values are within  $\pm 3N_i$ .

Fig. 5 shows the  $\Gamma_{crit}$  color contours on the contact surface for specimen #10. A crack nucleation site is predicted at the TE near the free surface of the specimen for both the  $\gamma_{crit}$  and  $\Gamma_{crit}$  models; this matches the location observed in the experiments [40].

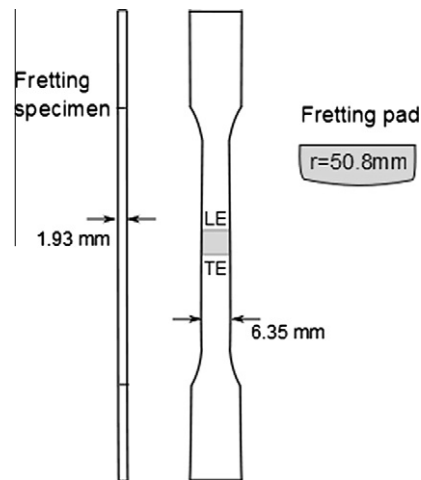


Fig. 4. Sketch of Lykins fretting specimen and pad [40].

**Table 1**  
Applied loading for Lykins' dog-bone specimens [40].

Specimen number	$S_{max}$ (MPa)	$S_{min}$ (MPa)	$Q_{max}$ (kN)	$Q_{min}$ (kN)
2	699.6	43.9	0.498	-0.316
6	424.6	35.2	0.547	-0.445
10	528.7	232.2	0.191	-0.214
11	686.6	455.8	0.472	0.12
18	410.1	273.2	0.467	0.125

**Table 2**  
 $G_{crit}$  nucleation model comparison – experimental versus predicted.

Specimen number	Lykins (experiment)		Predicted		$\gamma_{crit}$ Difference (%)	$N_i$ ratio
	$\gamma_{crit}$	$N_i$ (exp)	$\gamma_{crit}$	$N_i$		
2	9.96e-3	2.84e4	1.01e-2	3.67e4	-0.94	1.3
6	7.08e-3	8.27e4	0.71e-2	1.69e5	0.29	2.0
10	6.86e-3	2.36e5	0.64e-2	3.76e5	6.63	1.6
11	7.37e-3	3.34e5	0.63e-2	4.93e5	15.1	1.5
18	5.27e-3	4.50e7	0.44e-2	>1e9	17.1	-

**Table 3**  
SWT nucleation model comparison – experimental versus predicted.

Specimen number	Lykins (experiment)		Predicted		$\Gamma_{crit}$ Difference (%)	$N_i$ ratio
	$\Gamma_{crit}$	$N_i$ (exp)	$\Gamma_{crit}$	$N_i$		
2	3.79	2.84e4	3.73	3.07e4	1.67	1.1
6	2.08	8.27e4	2.04	1.19e5	1.69	1.4
10	1.81	2.36e5	1.77	1.89e5	2.05	0.8
11	1.92	3.34e5	1.70	2.20e5	11.3	0.7
18	1.06	4.50e7	0.87	>1e9	17.7	-

### 3.2. Analysis of dovetail test rig

A more advanced fretting fatigue test rig has been designed [34,44], which provides a more realistic comparison to a turbine engine blade/disk dovetail contact. A sketch of the fretting test specimen and pads is shown in Fig. 6 with the lower EOC (LE) labeled to help locate the crack nucleation site(s); the loading grips are not shown.

A 3D FE model of this test rig is built using ANSYS taking advantage of symmetry so that only half of the specimen and one fretting pad are modeled. The fretting surface is at a 45° orientation relative to the horizontal and vertical axes. The model is

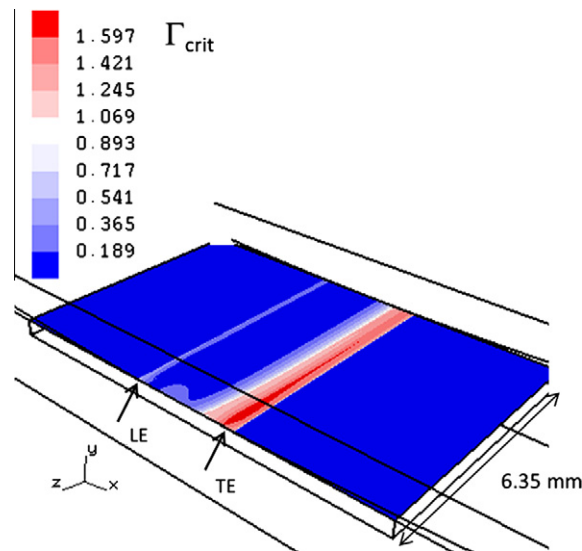


Fig. 5.  $\Gamma_{crit}$  Contour plot for specimen 10; maximum value is 1.77 MPa.

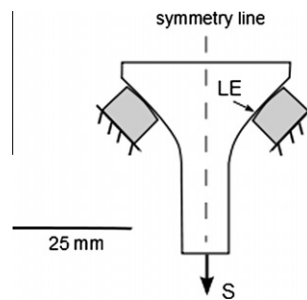


Fig. 6. Sketch of dovetail fretting test [34,44].

Table 4

Computed fretting nucleation parameters and cycles for dovetail test rig.

	(MPa)	$N_i$
$\gamma_{crit}$	0.011	2.71e4
$\Gamma_{crit}$	5.17	1.73e4
$\sigma_{eq}$	403	1.98e4

analyzed using two load steps, representing  $S_{max}$  and  $S_{min}$ . The fretting specimen and pad are both Ti–6Al–4V; the elastic modulus is 126.1 GPa, Poisson's ratio is 0.3, and the coefficient of friction on the contact surfaces is set to 0.3.

Based on the 16 experiments, Golden and Calcatera [34] have computed fretting fatigue crack nucleation lives between 5000 and 50,000 cycles. The maximum value of the fretting parameters and the corresponding predicted  $N_i$  are given in Table 4; the nucleation cycles fall within the above range. Fig. 7 shows the  $\sigma_{eq}$  color contours. The LE is the typical site of crack nucleation in the experiments [34]. The fretting nucleation models indicate different crack nucleation locations along this EOC. The  $\Gamma_{crit}$  and  $\sigma_{eq}$  models predict crack nucleation near the left end of the LE while the  $\gamma_{crit}$  model predicts crack nucleation near the right end. Golden and Calcatera [34] do not indicate a particular preferred crack nucleation site along the LE from the 16 tests, but have analyzed a surface elliptical crack at the specimen mid-thickness with a depth of 25  $\mu\text{m}$  and length of 125  $\mu\text{m}$ .

### 3.2.1. Crack growth simulation for dovetail test rig

A portion of the full ANSYS model was extracted for crack growth analysis, Fig. 8. An initial elliptical surface crack with dimensions of  $0.125 \times 0.025$  mm is inserted into the model at mid-specimen thickness at the LE (Fig. 9 – left panel). This initial crack is propagated for several steps to get an initial SIF history. Then a 0.25 mm deep edge crack is inserted along

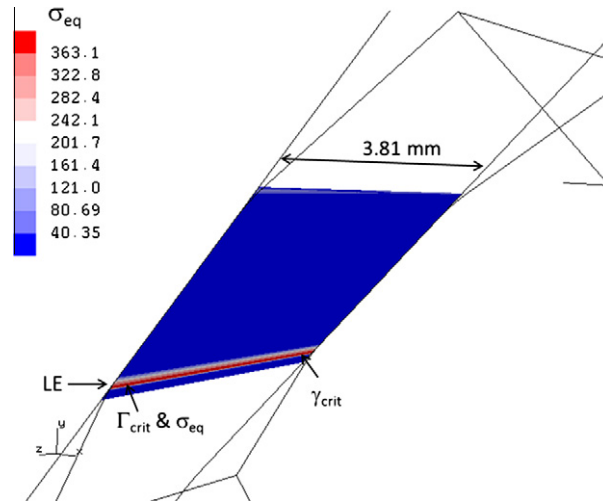


Fig. 7. Contour of parameter  $\sigma_{eq}$ ; maximum value is 403 MPa. Crack nucleation sites are predicted near the left and right ends of the lower EOC (LE).

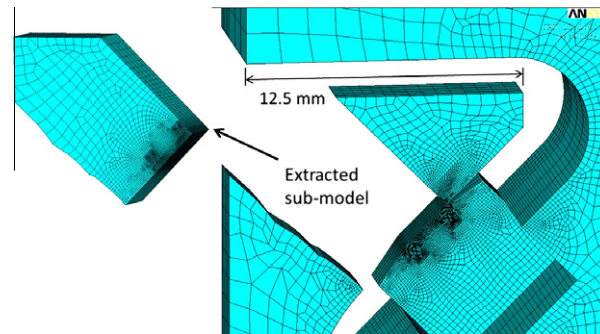


Fig. 8. FE model of dovetail fretting test rig with extracted sub-model.

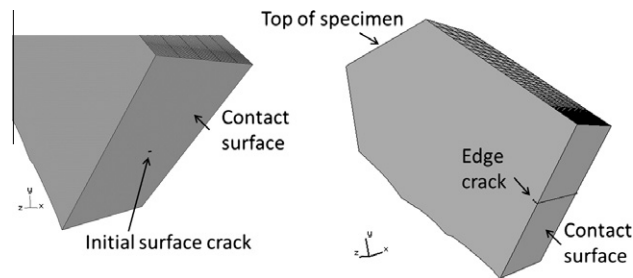


Fig. 9. Initial,  $0.125 \times 0.025$  mm surface crack (left panel) and subsequent 0.25 mm deep edge crack (right panel) in dovetail fretting specimen sub-model.

the entire length of the LE (Fig. 9 – right panel). This is done to simplify the subsequent crack growth simulation and to speed up the simulation as the ANSYS analysis for each crack growth step was taking up to 8 h. The initial edge crack is propagated for 35 steps at which point the crack front has almost reached the top of the specimen. The crack has grown to about 12 mm in length, as shown in the left panel of Fig. 10.

The observed surface trace of the crack from one of the tests is shown in the right panel of Fig. 10. The observed crack is approximately 10 mm long and inclined  $18^\circ$  from the normal to the contact surface. For the 16 tests, the observed angles varied from  $13^\circ$  to  $18^\circ$  [34]. The simulated crack is not a planar surface, but the average inclination is about  $16^\circ$ , which is in the observed range.

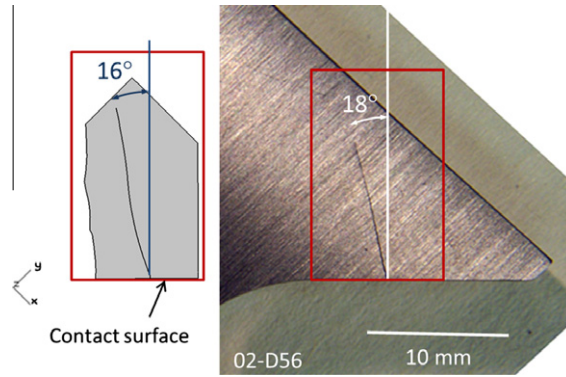


Fig. 10. Simulated (left panel) and observed (right panel – courtesy of Golden) crack path in dovetail fretting test rig specimen.

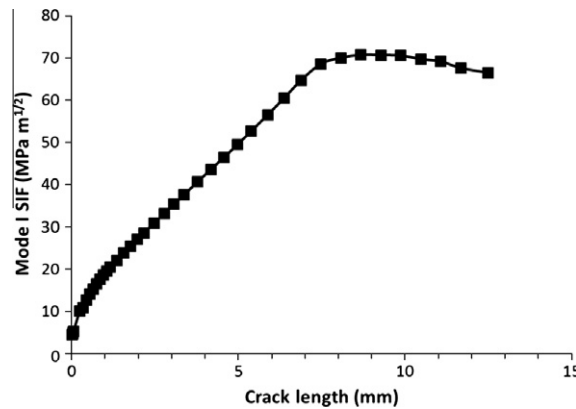


Fig. 11. Mode I SIF ( $K_{I_{max}}$ ) history for a crack in the dovetail fretting test rig model.

The Mode I SIF ( $K_{I_{max}}$ ) history is shown in Fig 11. The SIF history is computed along a path through the mid-points of the crack fronts. The Mode I SIF values begin to decrease as the crack front approaches the top of the specimen. The crack growth cycles can be computed using the appropriate Ti–6Al–4V crack growth rate data and the (AFRL) equation [34]:

$$\frac{da}{dN} = 0.0254 e^B \left(\frac{K_{eff}}{K_{th}}\right)^P \left[\ln\left(\frac{K_{eff}}{K_{th}}\right)\right]^Q \left[\ln\left(\frac{K_{eff}}{K_{th}}\right)\right]^d \tag{8}$$

where  $K_{eff} = K_{max}(1 - R)^m$  and  $R = K_{min}/K_{max}$ .  $K_{th}$ ,  $B$ ,  $P$ ,  $Q$ ,  $d$  and  $m$  are material dependent constants.

The resulting crack growth cycles are shown in Fig. 12. The loading is constant amplitude with  $R = 0.1$ , and the stress intensity range is above threshold ( $4.2 \text{ MPa m}^{1/2}$ ) for this material. The resulting number of discrete propagation cycles is approximately  $2.46e5$ . The predicted number of fretting nucleation cycles ranges from  $1.7e4$  to  $2.7e4$ . Thus the predicted total number of cycles is between  $2.63e5$  and  $2.73e5$ . This is consistent with the observed number of cycles in the experiments, which ranged from  $1e5$  to  $1e6$  [34].

This crack growth simulation was based on the maximum load. It was assumed that an  $R$  of 0.1 would be sufficient to keep the crack open at all times and this simplified the numerical modeling effort as crack face contact did not have to be imposed. It was assumed that  $K_{imin}/K_{Imax}$  would reflect this same  $R$  value. A more thorough analysis of the fatigue life and variation of  $K_{imin}/K_{Imax}$  with crack length is beyond the scope of this paper.

### 3.3. Analysis of turbine blade/disk dovetail

An ANSYS FE model of a single sector of a turbine blade/disk assembly is shown in Fig. 13. The blade and disk material are both Ti–6Al–4V with an elastic modulus of 126.1 GPa and Poisson’s ratio equal to 0.3. Loading consists of nodal temperatures and rotation, applied using five load steps. The load steps are defined at 50%, 72%, 110%, 72% and 50% of nominal loading.

The model has two sets of contact surfaces (pressure side and suction side) that must be considered during the fretting fatigue analysis. The coefficient of friction is set to 0.5 for both contact surfaces.

Fretting nucleation parameters are shown in Table 5, using load steps 3 and 1 as the maximum and minimum, respectively. The contour plot for the  $\sigma_{eq}$  parameter is shown in Fig. 14. The three fretting nucleation models predict different crack

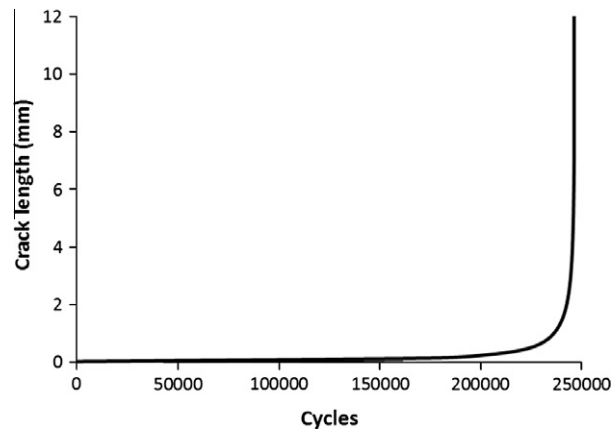


Fig. 12. Crack growth cycles for a crack in the dovetail fretting test rig model using the AFRL crack growth rate in Eq. (8).

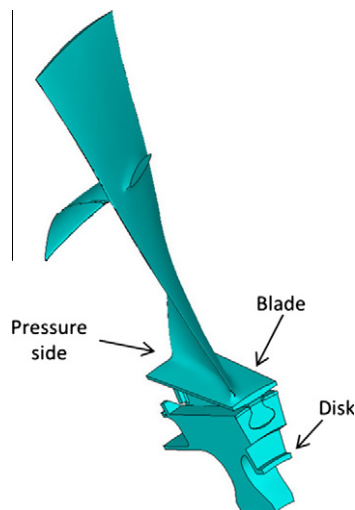


Fig. 13. FE model of a single sector blade/disk assembly.

**Table 5**  
Computed fretting nucleation parameters and cycles for the blade/disk dovetail model.

	(MPa)	$N_i$
$\gamma_{crit}$	0.015	1.32e4
$\Gamma_{crit}$	2.089	5.11e4
$\sigma_{eq}$	403	1.98e4

nucleation locations, as indicated in Fig. 14. The maximum  $\sigma_{eq}$  is located near the corner of the pressure side and forward face of the blade on the upper EOC. Relatively high values of  $\sigma_{eq}$  also exist midway along the upper EOC on the suction side of the blade. The maximum  $\gamma_{crit}$  is located on the suction side of the blade on the upper EOC at the corner of the aft face. The maximum  $\Gamma_{crit}$  value occurs in the disk rather than the blade, mid-way along the lower EOC on the suction side.

### 3.3.1. Simulated discrete cracking

Discrete crack growth simulations are performed at two locations on the blade, the nucleation sites predicted by the  $\sigma_{eq}$  and  $\gamma_{crit}$  models. Crack growth from other locations on the blade and disk could be analyzed, but this is beyond the scope of this paper. As shown in Fig. 14, the maximum  $\sigma_{eq}$  parameter is located on the blade, on the upper EOC, on the pressure side, near the forward face. A penny-shape (radius = 0.2 mm) surface crack is inserted at this location, Fig. 15, and then propagated; this location will be referred to as PBU.

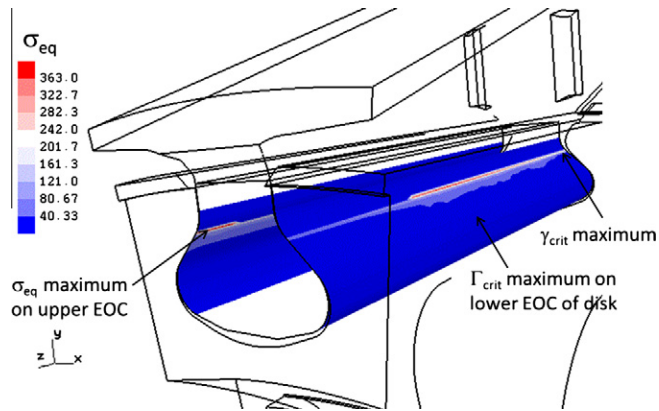


**Fig. 14.** Contour of parameter  $\sigma_{eq}$  on the blade surface.  $\sigma_{eq}$  Model predicts crack nucleation on pressure side of blade at the upper EOC,  $\gamma_{crit}$  model predicts crack nucleation on suction side of blade at the upper EOC, and  $\Gamma_{crit}$  model predicts crack nucleation on the suction side of the disk at the lower EOC (contours on disk not shown).

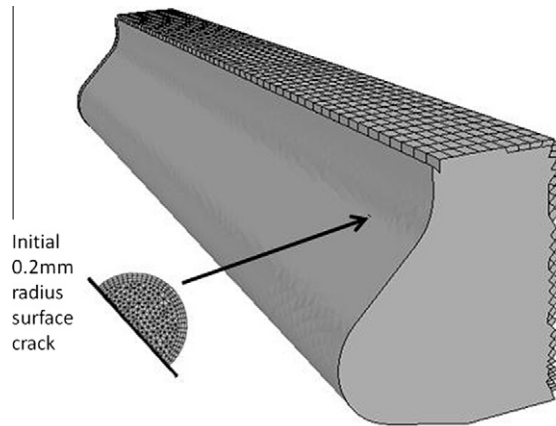


**Fig. 15.** Initial crack inserted at PBU location.

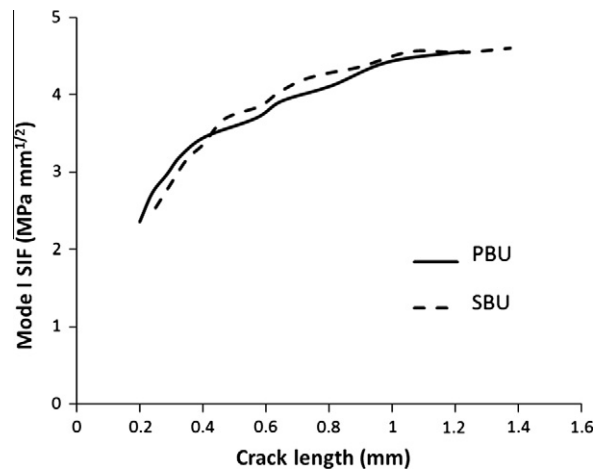


**Fig. 16.** Mode I SIF histories for PBU and SBU crack locations in blade/disk model.

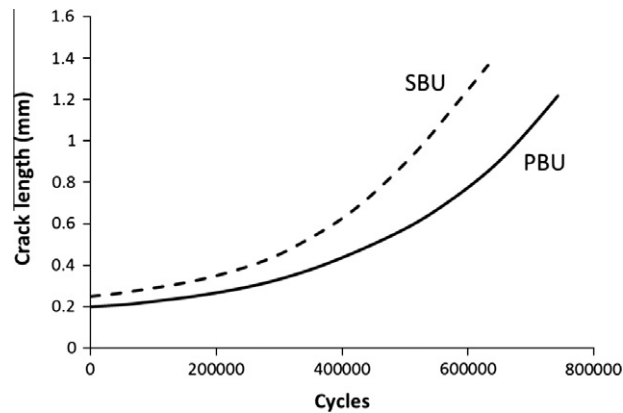


Fig. 17. Crack propagation cycles for PBU and SBU crack locations in blade/disk model.

As indicated in Fig. 14, the maximum  $\gamma_{crit}$  parameter is located on the blade dovetail surface, on the upper EOC, on the suction side, at the aft face corner. A penny-shape (radius = 0.25 mm) corner crack is inserted at this location also and then propagated; this location will be referred to as SBU.

### 3.3.2. Crack growth rate comparison

To compare the crack growth at the PBU and SBU locations, crack growth cycles are computed based on the respective SIF histories. Fig. 16 shows the Mode I SIF histories along a path through the mid-points of the two sets of crack fronts. The loading is constant amplitude loading with  $R = 0.2$ . The AFRL crack growth rate Eq. (8) is used to compute the number of cycles (Fig. 17). The two crack locations have similar Mode I SIF values and, therefore, have fairly similar crack growth rates. Based on the predicted crack nucleation and growth, it is likely that cracking will be observed in both locations. It is also possible that cracks will be observed in the disk based on the  $\Gamma_{crit}$  fretting model predictions.

### 3.3.3. Observed cracks

Barlow and Chandra [1] show images of cracks in the blade material and Enright et al. [45] show images of cracks in the disk. Crack growth simulations at all of the critical locations could be performed to determine the most critical location in terms of minimum fatigue life, but this is beyond the scope of the current study. Typically, multiple fretting cracks might nucleate along the EOC [1,46], and this is the focus of a separate study.

## 4. Discussion

The simulations in Section 3 illustrate the analysis methodology and the capabilities of the software for simulating the fretting fatigue crack nucleation and propagation process. However, it is clear that the prediction of fretting fatigue crack nucleation is rather imprecise. Fretting fatigue experiments provide a range of nucleation cycles along with a variety of crack locations (and possibly orientations). The numerical predictions typically fall within these ranges, but the data clearly calls for predictions that are realistically stochastic.

There are differences in the predictions from the various fretting nucleation models; this is expected as the models use different data and concepts. Four fretting nucleation models, available from the literature, have been implemented, and additional models could easily be included. An analyst can pick the one model that works best for the particular component geometry and material, or predict a range of fretting cycles and crack locations based on multiple models. As was shown in Sections 3.2 and 3.3, different fretting models might predict different crack nucleation locations, and it was shown in Section 3.1 that different fretting models can predict essentially identical crack nucleation locations but at different values of cycles. All the predictions fell within the experimental ranges, however.

Much of the data that enters into the numerical simulation is stochastic, including the component geometry. Small differences in contact surface dimensions and orientations could potentially lead to different results. Also, variations in the contact surface properties, in particular the friction coefficient, could lead to different predictions. These variations have not been systematically studied in this paper. However, the software described herein provides a suitable platform for performing these types of parametric sensitivity studies. Multiple FE analyses can be performed and the results quickly analyzed for fretting nucleation.

The available fretting nucleation models are essentially empirical, based on observations and measurements from experiments and correlated with computed numerical values. Some studies have focused on the micro-mechanical behavior of the contact surfaces, modeling discrete grains using elasto-plastic material models to determine the underlying mechanisms of fretting crack nucleation [47]. Micro-mechanical simulations, which use the FRANC3D software, are being performed at

Cornell University to study general fatigue mechanisms in metals [48,49]. These studies focus on correlating detailed microscopic images of fatigue crack incubation and nucleation in an aluminum alloy subjected to cyclic loading. The observed fatigue cracking on the specimen surface along with the load history was replicated in numerical simulations to arrive at better physics-based mathematical models for crack nucleation. This same approach could be extended to study fretting fatigue crack nucleation, where the crack nucleation process will include the surface-to-surface contact mechanisms. However, direct observation of the contact surface during testing usually is not possible, and it might be difficult to reproduce results when doing start–stop type testing due to the potential loss of trapped wear debris when separating the in-contact components and because the local slip history will be disturbed.

## 5. Observations and conclusions

This work describes an innovative approach for integrating existing fretting fatigue crack nucleation models, off-the-shelf commercial finite element software, and discrete crack growth simulation capabilities to compute total fatigue life for components that are in contact with limited slip or sliding.

Fretting fatigue crack nucleation and subsequent propagation is simulated in 3D using standard commercial finite element software (in this case ANSYS), along with a 3D fracture analysis simulation program, FRANC3D. Four fretting nucleation models, available from the literature, are implemented to provide an analyst with a prediction of fretting nucleation cycles and initial crack location. The selection of the fretting model relies on user preference and experience; alternatively, multiple models can be selected to provide a range of predictions. Subsequent discrete crack growth is simulated with the combined software to provide SIF histories and propagation cycles. The total fretting fatigue life is the sum of the fretting nucleation and the discrete crack propagation cycles.

The software and the simulation procedure have been validated against experimental data for both fretting crack nucleation and subsequent discrete crack growth. Fretting cycles and crack nucleation sites match those observed in typical fretting experiments, as shown in Section 3.1. For this fretting test, the predicted number of fretting cycles based on the  $\gamma_{crit}$  and  $\Gamma_{crit}$  fretting models falls within the experimental scatter, and the predicted crack location near the free surface at the trailing edge of contact matches well with experimental observations. For fretting test specimens that more closely resemble turbine engine blade/disk components, predictions of fretting nucleation cycles and discrete crack propagation cycles also fall within experimental observations, as shown in Section 3.2. In addition, the discrete crack growth trajectory closely resembles that from the experiments.

The goal of the software development was to provide a framework for quickly and easily modeling the fretting fatigue process in actual turbine engine hardware. As shown in Section 3.3, using an existing FE model of a blade/disk assembly, fretting cycles and nucleation sites are predicted that are comparable to observations from the field. These predictions might be adequate for an engineering analysis; however, the stochastic nature of the data and the imprecision of the predictions indicate that a more fundamental understanding of the fretting process is required as a basis for accurate, stochastic, case-independent simulations. Micro-mechanical software tools could be used to simulate the fretting nucleation process to gain a better understanding of the underlying physical mechanisms. This potentially could reduce the uncertainty in predicting the number of cycles and fretting crack nucleation, leading to more accurate predictions of total fatigue life.

## Acknowledgments

The authors would like to thank Dr. Pat Golden at AFRL, Wright Patterson Air Force Base for supplying the data, drawings and finite element models for the dovetail fretting tests. The authors would also like to thank Dr. Jalees Ahmad for his assistance with the crack analog fretting model. This work was funded by a US Navy SBIR contract (#N68335-08-C-0011).

NAVAIR Public release 11-1662.

Distribution: Statement A – “Approved for public release; distribution is unlimited”.

## References

- [1] Barlow KW, Chandra R. Fatigue crack propagation simulation in an aircraft engine fan blade attachment. *Int J Fatigue* 2005;27:1661–8.
- [2] Barella S, Boniardi M, Cincera S, Pellin P, Degive X, Gijbels S. Failure analysis of a third stage gas turbine blade. *Engng Fail Anal* 2011;18:386–93.
- [3] Krishnakumar S, Dhamari R. Fatigue behaviour of aluminium alloy 7075 bolted joints treated with oily film corrosion compounds. *Mater Des* 2002;23:209–16.
- [4] Santus C. Fretting fatigue of aluminum alloy in contact with steel in oil drill pipe connections, modeling to interpret test results. *Int J Fatigue* 2008;30:677–88.
- [5] Hyde TR, Leen SB, McColl IR. A simplified fretting test methodology for complex shaft couplings. *Fatigue Fract Engng Mater Struct* 2005;28:1047–67.
- [6] Ding J, Sum WS, Sabesan R, Leen SB, McColl IR, Williams EJ. Fretting fatigue predictions in a complex coupling. *Int J Fatigue* 2007;29:1229–44.
- [7] Ekberg A. Fretting fatigue of railway axles – a review of predictive methods and an outline of a finite element model. *Proc Inst Mech Eng Part F – J Rail Rapid Transit* 2004;218:299–316 [Special issue paper].
- [8] Luo DB, Fridrici V, Kapsaa P. Selecting solid lubricant coatings under fretting conditions. *Wear* 2010;268:816–27.
- [9] Murthy H, Mseis G, Farris TN. Life estimation of Ti–6Al–4V specimens subjected to fretting fatigue and effect of surface treatments. *Tribol Int* 2009;42:1304–15.
- [10] Ruiz C, Boddington PHB, Chen KC. An investigation of fatigue and fretting in a dovetail joint. *Exp Mech* 1984;24:208–17.
- [11] Szolwinski MP, Farris TN. Mechanics of fretting fatigue crack formulation. *Wear* 1996;198:93–107.
- [12] Golden PJ, Grandt AF. Fracture mechanics based fretting fatigue life predictions in Ti–6Al–4V. *Engng Fract Mech* 2004;71:2229–43.

- [13] Lykins CD, Mall S, Jain VK. A shear stress based parameter for fretting fatigue crack initiation. *Fatigue Fract Engng Mater Struct* 2001;24:461–74.
- [14] Arrieta HV, Wackers P, Dang Van K, Constantinescu A. Modelling attempts to predict fretting-fatigue life on turbine components. RTO-MP-AVT-109. 2002;22-1–22-12.
- [15] Hattori T, Nakamura M, Watanabe T. Simulation of fretting-fatigue life by using stress-singularity parameters and fracture mechanics. *Tribol Int* 2003;36:87–97.
- [16] Ahmad J, Santhosh U. Methodology for fretting fatigue damage and life prediction of turbine engine components. Phase II SBIR Final Report 2006. Contract N68335-03-C-0085.
- [17] Ciavarella M. A crack-like notch analogue (CLNA) for a safe-life fretting fatigue design methodology. *Fatigue Fract Engng Mater Struct* 2003;26:1159–70.
- [18] Giannakopoulos AE, Lindley TC, Suresh S. Aspects of equivalence between contact mechanics and fracture mechanics: theoretical connections and life-prediction methodology for fretting-fatigue. *Acta Mater* 1998;46:2955–68.
- [19] Hills DA, Nowell D. *Mechanics of fretting fatigue*. Dordrecht: Kluwer; 1994. 236p.
- [20] Naboulsi S, Calcaterra J. Fretting fatigue investigation of dovetail. In: 11th Int conf fract. Turin, Italy; 2005.
- [21] Chan KS, Lee Y, Davidson DL, Hudak SJ. A fracture mechanics approach to high cycle fretting fatigue based on the worst case fret concept. *Int J Fract* 2001;112:299–330.
- [22] Iyer K, Mall S. Analyses of contact pressure and stress amplitude effects on fretting fatigue life. *J Engng Mater Technol* 2001;123:85–93.
- [23] Lykins CD, Mall S, Jain VK. An evaluation of parameters for predicting fretting fatigue crack initiation. *Int J Fatigue* 2000;22:703–16.
- [24] Garcia DB, Grandt AF. Application of a total life prediction model for fretting fatigue in Ti–6Al–4V. *Int J Fatigue* 2007;29:1311–8.
- [25] Fouvry S, Kapsa P, Sidoroff F, Vincent L. Identification of the characteristic length scale for fatigue cracking in fretting contacts. *J de Phys IV* 1998;8:159–66.
- [26] Araujo JA, Nowell D, Vivacqua RC. The use of multiaxial fatigue models to predict fretting fatigue life of components subjected to different contact stress fields. *Fatigue Fract Engng Mater Struct* 2004;27:967–78.
- [27] Ciavarella M, Demelio GP. A review of analytical aspects of fretting fatigue, with extension to damage parameters, and application to dovetail joints. *Int J Solids Struct* 2001;38:1791–811.
- [28] Faanes S. Inclined cracks in fretting fatigue. *Engng Fract Mech* 1995;52:71–82.
- [29] Fadag HA, Mall S, Jain VK. A finite element analysis of fretting fatigue crack growth behavior in Ti–6Al–4V. *Engng Fract Mech* 2008;75:1384–99.
- [30] Fouvry S, Nowell D, Kubiak K, Hills DA. Prediction of fretting crack propagation based on a short crack methodology. *Engng Fract Mech* 2008;75:1605–22.
- [31] Fouvry S, Kubiak K. Introduction of a fretting-fatigue mapping concept: development of a dual crack nucleation – crack propagation approach to formalize fretting-fatigue damage. *Int J Fatigue* 2009;31:250–62.
- [32] Baietto MC, Pierres E, Gravouil A. A multi-model X-FEM strategy dedicated to frictional crack growth under cyclic fretting fatigue loadings. *Int J Solids Struct* 2010;47:1405–23.
- [33] Proudhon H, Basseville S. Finite element analysis of fretting crack propagation. *Engng Fract Mech* 2011;78:685–94.
- [34] Golden PJ, Calcaterra JR. A fracture mechanics life prediction methodology applied to dovetail fretting. *Tribol Int* 2006;39:1172–80.
- [35] Navarro C, Garcia M, Dominguez J. A procedure for estimating the total life in fretting fatigue. *Fatigue Fract Engng Mater Struct* 2003;26:459–68.
- [36] Giner E, Navarro C, Sabsabi M, Tura M, Dominguez N, Fuenmayor FJ. Fretting fatigue life prediction using the extended finite element method. *Int J Mech Sci* 2011;53:217–25.
- [37] Pierres E, Baietto MC, Gravouil A, Morales-Espejel G. 3D two scale X-FEM crack model with interfacial frictional contact. *Tribol Int* 2010;40:1831–41.
- [38] ANSYS is a registered trademark of Ansys, Inc., <<http://www.ansys.com/>>.
- [39] Wawrzyniek PA, Carter BJ, Ingrassia AR. Advances in simulation of arbitrary 3D crack growth using FRANC3D/NG. In: Proceedings of the 12th international conference on fracture. Ottawa; 2009.
- [40] Lykins CD. An investigation of fretting fatigue crack initiation behavior on the titanium alloy Ti–6Al–4V. PhD thesis. University of Dayton; 1999.
- [41] Russ SM, Rosenberger AH, Larsen JM, Berkley RB, Carroll D, Cowles BA, Holmes RA, Littles JW, Pettit RG, Schirra JJ. Demonstration of advanced life-prediction and state-awareness technologies necessary for prognosis of turbine engine disks. Health monitoring and smart nondestructive evaluation of structural and biological systems III. In: Tribikram Kundu, editor. Proceedings of SPIE, 5394. Bellingham, (WA): SPIE; 2004. p. 23–32.
- [42] Paris PC, Erdogan F. A critical analysis of crack propagation laws. *J Basic Engng; Trans ASME, Ser D* 1963;85:528–34.
- [43] NASGRO reference manual. Version 4.02, September 2002, Southwest Research Institute; <<http://www.nasgro.com/>>.
- [44] Golden PJ. Development of a dovetail fretting fatigue fixture for turbine engine materials. *Int J Fatigue* 2009;31:620–8.
- [45] Enright MP, Chan KS, Moody JP, Golden PJ, Chandra R, Pentz AC. Probabilistic fretting fatigue assessment of aircraft engine disks. *J Engng Gas Turbines Power* 2010;132:072502-1–2-9.
- [46] Farris TN. Micromechanics analysis of fretting fatigue. In: Leon keer symposium. Syms; 2010.
- [47] Zhang M, Neu RW, McDowell DL. Microstructure-sensitive modeling: application to fretting contacts. *Int J Fatigue* 2009;31:1397–406.
- [48] Veilleux MG. Geometrically explicit finite element modeling of AA7075-T651 microstructure with fatigue cracks. PhD dissertation. Cornell University; 2010.
- [49] Hochhalter JD. Finite element simulations of fatigue crack stages in AA7075-T651 microstructure. PhD dissertation. Cornell University; 2010.